Energy-saving potential of dedicated outdoor-air system assisted by vacuum-based membrane dehumidifier

Seong-Yong Cheon[1], *Soo-Yeol* Yoon[1], *Su* Liu[1], and *Jae-Weon* Jeong[1,*]

[1]Department of Architectural Engineering, Hanyang University, Republic of Korea.

Abstract. The proposed research presents a dedicated outdoor-air system (DOAS) integrated with a vacuum-based membrane dehumidifier (VMD). The primary objective of this study was to evaluate the energy-saving potential of the proposed VMD–DOAS combination. VMD–DOAS comprised a membrane-energy exchanger (MEE), dew-point indirect evaporative cooler (DP-IEC), and VMD. VMD possessed a characteristic by virtue of which the dehumidification process was isothermal; i.e., no temperature change was observed during the VMD process. While VMD served to control the dry-air supply, the required target temperature (i.e., 17 °C) was maintained via DP-IEC operation. The remaining sensible heat of the conditioned zone was controlled by the ceiling radiant cooling panel (CRCP). The load of the conditioned zone was driven by TRANSYS 18, and an engineering equation solver (EES) was used for evaluating the energy-saving potential of the proposed system with CRCP by comparing it against the variable-air-volume (VAV) system. Results of this study demonstrated that the proposed DOAS with CRCP consumed 37% less operating energy compared to the VAV system. This observed energy-saving potential of the proposed system was driven by reducing the dehumidification load and subsequent energy recovery by MEE.

1 Introduction

Numerous studies concerning dedicated outdoor-air systems (DOAS) in combination with a ceiling radiant cooling panel (CRCP) have previously been performed and their results applied to buildings [1, 2]. DOAS provides ventilation and humidity control, whereas CRCP is responsible for providing sensible cooling within the conditioned zone as a decoupling system capable of enhancing the indoor environmental quality while also saving energy. Various dehumidification devices integrated with DOAS have recently been proposed to enhance humidity-control and energy-saving effects of such systems [3, 4].

Vacuum-based membrane dehumidifier (VMD) is a promising dehumidifier type, and it has attracted considerable attention owing to its characteristic of performing isothermal dehumidification [5]. VMD simplifies the dehumidification process by removing only water vapor without effecting any change in the supply-air temperature. Extant researches [6, 7] have demonstrated the utility of VDM-assisted air-cooling systems via simulations as well as experiments. Eldessouky et al. [6] proposed a numerical method for analyzing air-cooling systems comprising VMD and an evaporative cooler. When the evaporative cooler was operated under humid outdoor-air conditions, VMD was used to remove water vapor from the process air. Lin et al. [7] proposed a hybrid cooling system comprising VMD in combination with a dew-point evaporative cooler, and they investigated the capability of the hybrid cooling system through experiments. Their results demonstrated that utility of the said hybrid cooling system was improved when used in combination with VMD, which served to eliminate water vapor, when compared against a solitary-stage dew-point evaporative cooler.

This study proposes use of a vacuum-based membrane dehumidifier in combination with a dedicated outdoor-air system (VMD–DOAS). To estimate the operational feasibility of the proposed system, energy consumption of the same was evaluated via comparison against a variable-air-volume (VAV) system as a conventional HVAC unit.

2 System overview

2.1. Variable-air-volume (VAV) system

Figure 1 depicts a schematic of the conditioned zone served by a VAV system, wherein the supply-air flow rate is set by the value of a sensible load of the conditioned zone. To reduce the cooling coil load for reducing energy consumption, a certain minimum amount of ventilation, which corresponds to outdoor air (OA), is mixed with the return air (RA). Cooling and heating modes of a VAV system are determined by the sensible and latent loads of the conditioned zone. In the cooling mode, the supply air is cooled and dehumidified by the cooling coil, and subsequently, the heating coil is operated to attain the target temperature (i.e., 13 °C) as required. In the heating

* Corresponding author: jjwarc@hanyang.ac.kr

mode, the supply-air temperature is controlled to meet the neutral temperature (i.e., 20 °C) by the heating coil, and the remaining sensible heating load is dealt with via use of a parallel heating unit. When operating during the intermediate season, the VAV system is commonly employed as an airside economizer to reduce the cooling load. The supply-air dry-bulb temperatures are set at 13 °C and 20 °C in the cooling and heating modes, respectively.

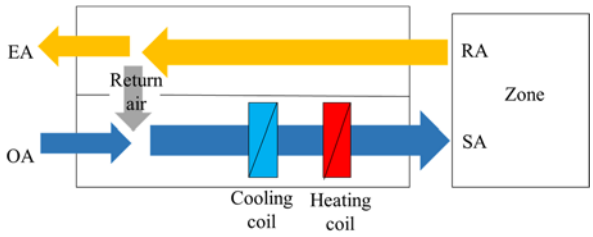

Fig. 1. Variable-air-volume (VAV) system.

2.2 Proposed VMD–DOAS

In the proposed system, the dedicated outdoor-air system (DOAS) supplies dehumidified minimum-ventilation air and accommodates all latent loads of the conditioned zone; additionally, a part of the sensible-cooling load could be reduced by the supply-air temperature of DOAS.

Figure 2 depicts a schematic of the proposed VMD–DOAS equipped with CRCP. The proposed system comprised a membrane-energy exchanger (MEE), VMD, and dew-point indirect evaporative cooler (DP-IEC). MEE was operated for pre-conditioning the outdoor air by recovering energy from exhaust air. When the available process air is too humid to be supplied to the conditioned zone, VMD is operated to remove moisture from the process air. The VMD operation is based on the pressure difference between the process air stream and vacuum side. When air temperature at the process inlet exceeds that within the conditioned zone, DP-IEC is operated for controlling the supply-air temperature to within 17 °C by means of evaporative cooling. The remaining sensible cooling load is dealt with through use of CRCP as a parallel cooling device.

When the conditioned zone requires heating, the proposed DOAS is operated to supply the minimum ventilation air flow rate at the neutral temperature (20°C), and the heating load of the conditioned zone is dealt with via use of a parallel heating device.

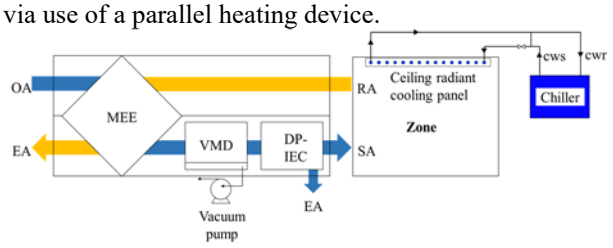

Fig. 2. Proposed VMD–DOAS with ceiling radiant cooling panel (CRCP).

2.3 Modes of operation

In the proposed DOAS, operating modes are classified into three different types based on outdoor-air conditions. As depicted in Figure 3, when the enthalpy and humidity ratios of the outdoor air exceed those of the air within the conditioned zone (i.e., region 1), MEE is operated to precool and predehumidify the intake outdoor air by recovering energy from exhaust air. VMD additionally dehumidifies the process air as it passes through MEE, thereby satisfying the humidity ratio requirement. When the dry-bulb temperature of the outdoor air exceeds room temperature, DP-IEC is operated for cooling the process air to at least the room temperature (25 °C). Because DP-IEC operation requires additional air flow rate for evaporative cooling owing to it being a regenerative indirect cooler, a portion of the process air must be introduced to operate the cooling device.

When enthalpy of the outdoor air is lower compared to that of air at room temperature while its corresponding humidity ratio exceeds the target humidity ratio of supply air (i.e., region 2), MEE is not operated, but is rather bypassed, to prevent an increase in intake outdoor enthalpy. VMD is operated to dehumidify the intake outdoor air to meet the target supply-air humidity ratio. Similar to region 1, operation of DP-IEC is determined by comparing dry-bulb temperatures of the outdoor and room air.

When the humidity ratio of outdoor air is lower compared to the target humidity ratio, MEE is operated by recovering energy from exhaust air. VMD is not operated. If the outdoor-air temperature exceeds room temperature, DP-IEC is operated for the cooling device. While the outdoor-air temperature is lower compared to the room temperature, the supply-air temperature is brought to the neutral value (20 °C) by the electric heater. The operational logic of system components is described in Figure 4.

Because the proposed DOAS acts as a ventilator for conditioning latent loads of the conditioned zone, parallel cooling and heating devices are needed to treat sensible loads of the conditioned zone. When the remaining sensible cooling load manifests, it is treated by CRCP as the cooling device. When sensible heating load occurs, a parallel heating device, such as an electric fan coil unit, is employed.

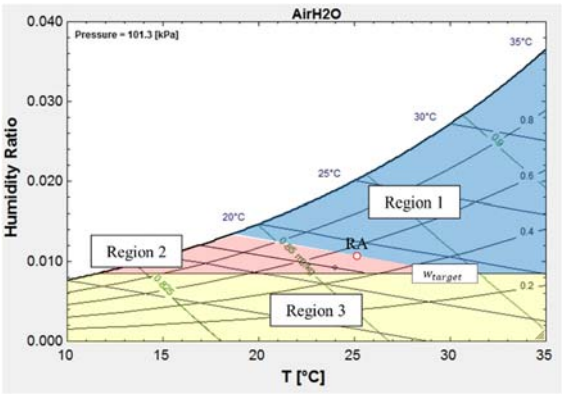

Fig. 3. Operating modes of proposed DOAS plotted on psychrometric chart.

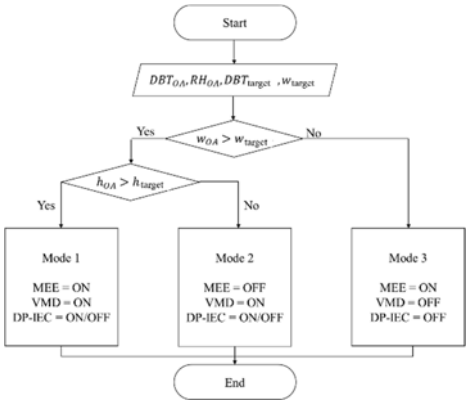

Fig. 4. Operational logic of proposed DOAS.

3 Simulation setup and overview

3.1 Model space

Sensible and latent loads were simulated using the TRNSYS 18 program. The building model considered in this study comprised a 400-m^2 office. Windows were located on the south-facing wall, and the window-to-wall ratio equaled 0.17. Sensible and latent heats of occupants were set equal to 70 W/person and 45 W/person, respectively. U-values of the exterior condition were determined based on the local energy-conservation building code. Target conditions of the conditioned zone were assumed to be 25 °C with 55% relative humidity during cooling and 20 °C during heating. Detailed parameters of the building model are described in Table 1.

Table 1. Physical conditions of model space.

Location	Seoul, South Korea	
Geometry	20 × 20 × 3 m (W × L × H)	
U-values	Roof, Ceiling	0.297 W/m^{2}K
	Wall	0.257 W/m^{2}K
	Windows	1.4 W/m^{2}K
Internal heat gain	Equipment	140 W/person
	Occupant	70 W/person (Sensible)
		45 W/person (Latent)
	Light	13 W/m^2
Room set point	Cooling	Temperature : 25 °C
		RH : 55%
	Heating	Temperature : 20 °C
		RH :

3.2 System component models

3.2.1 Membrane-energy exchanger

In DOAS, the supply-air flow rate is defined as the minimum required outdoor-air flow rate based on the number of occupants and space size. An enthalpy exchanger can be employed to recover energy from exhaust air via use of an MEE. The outlet temperature and humidity ratio of the process air passing through the MEE could be determined using equations (1) and (2), respectively. When DP-IEC is operated, flow rate of the supply air exceeds that of return air, and the outlet temperature and humidity ratio are considered to prevail under an unbalanced flow condition. The sensible and latent heat-exchange effectiveness of MEE were assumed to possess values of 0.7 and 0.6, respectively, in accordance with [8].

$$T_{pro,out} = T_{OA} - eff_{sen}\frac{\dot{m}_{OA}C_{p,a}(T_{OA}-T_{RA})}{\dot{m}_{RA}C_{p,a}} \quad (1)$$

$$w_{pro,out} = w_{OA} - eff_{lat}\frac{\dot{m}_{OA}C_{p,a}(w_{OA}-w_{RA})}{\dot{m}_{RA}C_{p,a}} \quad (2)$$

3.2.2 Vacuum-based membrane dehumidifier

VMD, in this study, was operated for dehumidifying the process air to meet the target humidity ratio requirement. VMD dehumidifies the process air in accordance with the pressure differential between the feed and permeate sides, as depicted in Figure 5. When a pressure differential is imposed between the feed and permeate sides via use of a vacuum pump, water vapor permeates through the membrane layer. Then, the process air exclusively comprises dry air, and water vapor on the permeate side is flushed out through the vacuum pump.

To estimate the performance and energy consumption of the VMD system proposed in this study, an existing black-box model was used [9]. The VMD model predicted the dehumidification efficiency (DE), which relates the dry-bulb temperature and relative humidity via equation (3). The dehumidification rate of the above-described VMD module was determined using equation (4). The membrane surface area ($A_{membrane}$) equaled 38.4 m^2, and VMD power equaled 300 W when the supply air flow rate was 240 kg/h. The total VMD energy consumption was determined in terms of a proportional increase in the supply-air flow rate through VMD–DOAS.

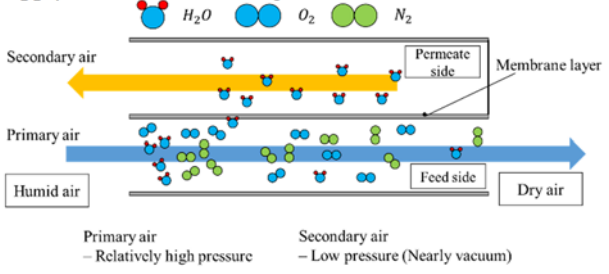

Fig. 5. Configuration of vacuum-based membrane dehumidifier.

$$DE = -20 + 1.18t_{in} + 0.02t_{in}^2 + 0.0003\mathrm{RH}_{in} - 0.0002RH_{in}^2 + 0.0003t_{in}RH_{in} \quad (3)$$

$$\Delta w = DE * (A_{membrane} \times P_{VMD})/\dot{m}_{VMD} \quad (4)$$

3.2.3 Dew-point indirect evaporative cooler

In Figure 6, DP-IEC was operated for cooling the process air to meet the supply-air target temperature requirements. The temperature of the supply air at inlet exceeded room temperature. In this case, the ratio of the air flow rate between the primary and secondary outlets was set at 7:3 to encourage evaporative cooling. The remainder of the process air was supplied to the conditioned zone to satisfy the minimum ventilation flow rate requirement. When operating DP-IEC for cooling, approximately 30% more outdoor air compared to the minimum ventilation requirement must be drawn in. While the supply air requires heating, the DP-IEC operation is terminated by blocking the secondary air stream. The outlet-air temperature after DP-IEC operation could be predicted using the modified ε-NTU method given by equations (5) through (9). A simplified DP-IEC model was developed using experimental data reported in [10].

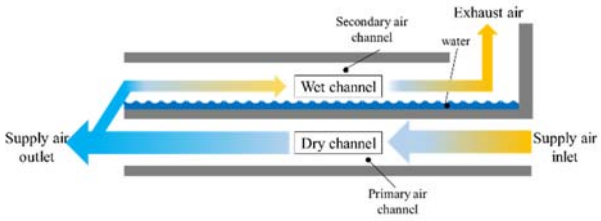

Fig. 6. Configuration of dew-point indirect evaporative cooler.

$$T_{pro,out} = T_{pro,in} - \frac{\mathrm{Q}_{IEC}}{\mathrm{C}_h} \quad (5)$$

$$T_{sec,out}^{wb} = T_{sec,in}^{wb} + \frac{\mathrm{Q}_{IEC}}{\mathrm{C}_c} \quad (6)$$

$$\mathrm{Q}_{max} = C_{min}(T_{pro,in} - T_{s,in}^{wb}) \quad (7)$$

$$\varepsilon_{IEC} = \frac{1-\exp(-NTU(1-C_r)}{1-C_r\exp(-NTU(1-C_r))} \quad (8)$$

$$\mathrm{Q}_{IEC} = \varepsilon_{IEC}\mathrm{Q}_{max} \quad (9)$$

3.2.4 Electric chiller and heater models

In both the VAV and CRCP systems, the chiller model comprised the air-cooled chiller model of DOE-2 [11] to determine the energy consumption of respective systems via equations (10) through (14). The said model requires four performance curves to determine the total power consumed by the chiller. The said curves include those corresponding to the available cooling capacity of the chiller (CAPFT), energy input corresponding to the cooling output factor (EIRFT), part-load efficiency of the chiller (EIRFPLR), and part load ratio (PLR).

$$CAPFT = f(T_{CWS}, T_{OA}) \quad (10)$$

$$EIRFT = f(T_{CWS}, T_{OA}) \quad (11)$$

$$EIRFPLR = f(PRL) \quad (12)$$

$$PLR = \frac{Required\ cooling\ load}{Capacity\ of\ chiller \cdot CAPFT} \quad (13)$$

$$P_{chiler} = P_{ref} \cdot CAPFT \cdot EIRFT \cdot EIRFPLR \quad (14)$$

The heating load of the conditioned zone and heating process for heating and reheating in each system were accommodated by an electric heating coil as the parallel heating unit. The electric coils were adopted for conditioning the air in all the heating coils and energy consumption is calculated by Equations (15) to (17).

$$P_{h,coil} = \dot{Q}_{h,coil} \quad (15)$$

$$P_{reh,coil} = \dot{Q}_{reh,coil} \quad (16)$$

$$P_{h,parallel} = \dot{Q}_{h,parallel} \quad (17)$$

3.2.5 Ceiling radiant cooling panel

In the proposed VMD–DOAS with CRCP, CRCP is operated for removing the remaining sensible cooling load that could not be handled by the proposed DOAS in the conditioned zone as a parallel cooling device. As depicted in Figure 2, cold water at the exit of the chiller was supplied to CRCP, and the same was used to remove with the remaining sensible-cooling load. The corresponding CRCP load is defined by Equation (15).

$$\mathrm{Q}_{CRCP} = \mathrm{Q}_{c,sen,zone} - Q_{sen,DOAS} \quad (15)$$

4 Results

4.1 Seasonal energy consumption

4.1.1 Summer (June–August)

Figure 7 depicts the comparison of the primary-energy consumption of the proposed DOAS with CRCP and VAV system when operating during summer. It can be seen that the proposed system consumed 12% more energy compared to the VAV system during summer. As regards the dehumidification of process air, the proposed VMD-based system demonstrated 24% lower latent load compared to the VAV system. Although the latent load for dehumidifying outdoor air was reduced when using VMD, the total energy consumed when handling the sensible and latent loads was observed to be higher for the proposed system owing to the lower coefficient of performance (COP) of VMD compared to the chiller.

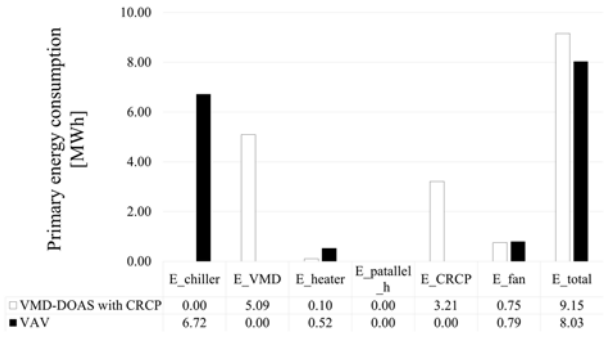

Fig. 7. Comparison of primary energy consumption of candidate systems during summer.

4.1.2 Intermediate season (March–May and September–November)

Figure 8 depicts comparison of the primary energy consumed by the proposed DOAS with the CRCP and VAV system during the intermediate season. It can be realized that the proposed system demonstrated 40% savings in terms of primary-energy consumption compared to the VAV system during the intermediate season. The main energy-saving potential of the proposed system was driven by the MEE operation, which recovers heat from return/exhaust air, thereby resulting in up to 60% less energy consumption compared to the electric heater.

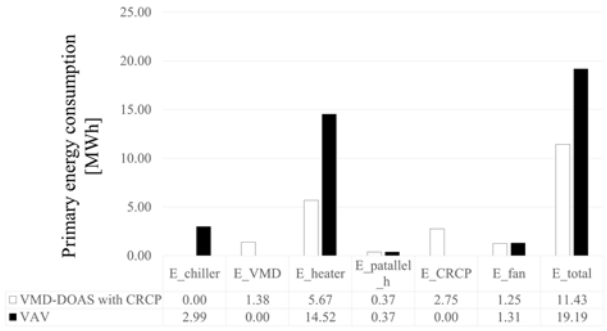

Fig. 8. Comparison of primary energy consumption of candidate systems during the intermediate season.

4.1.3 Winter (December–February)

As depicted in Figure 9, VMD was not operated during winters, because the humidity ratio of outdoor air was lower compared to the target humidity ratio in winter. The candidate system, therefore, operated to exclusively heat the supply air to meet the target temperature requirement of 20°C. In the proposed DOAS, the supply-air temperature was controlled by MEE as the preheating device. Major energy savings were realized in terms of electric-heater energy consumption (i.e., 70% less energy consumed by the electric heater) to meet the neutral temperature requirement. It is shown that use of the proposed system led to 53% savings in terms of primary energy consumption compared to the VAV system during winters.

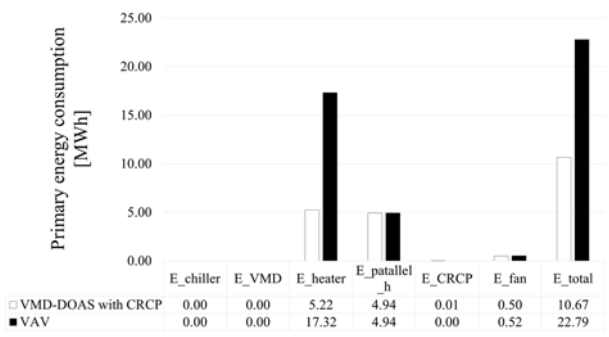

Fig. 9. Comparison of primary energy consumption of candidate systems during winter.

4.2 Annual energy consumption

Figure 10 depicts a comparison of the annual consumption of primary energy by the proposed and VAV systems. The average COP of the chiller was 3.3 but that of the VMD was 1.98. While the proposed system reduced the dehumidification load by using VMD, which performed an isothermal dehumidification process, the total energy consumed in handling the total sensible and latent load was observed to be more in the proposed system owing to the lower COP of VMD compared to the chiller. In heating mode, the MEE, which is integrated with proposed DOAS, reduces the energy of the electric heater by recovering heat from the return air. As can be realized from the figure, use of the proposed system results in annual savings of 37% with regard to primary energy consumption when compared to the VAV system.

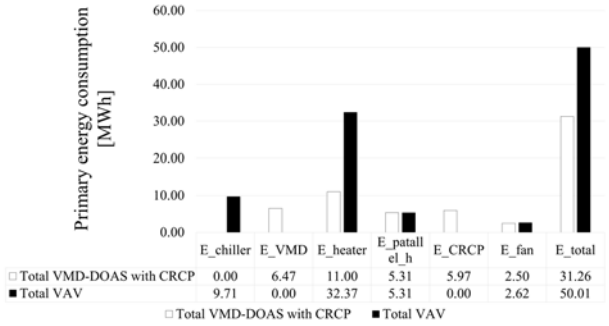

Fig. 10. Comparison of annual primary energy consumption of the proposed DOAS against VAV system.

5 Conclusions

This study proposes use of an integrated VMD–DOAS to reduce the dehumidification load by means of an isothermal dehumidification process. To determine the operational energy consumption of the proposed DOAS, energy consumed by the proposed DOAS was compared against those consumed by the CRCP and VAV systems, values of each of which were simulated using EES. Based on simulations results obtained in this study, it can be inferred that use of the proposed VMD–DOAS integrated with CRCP leads to 37% greater annual energy savings compared to conventional VAV systems. The

dehumidification load of the proposed system is reduced by 33% owing to the use of VMD to meet the target humidity ratio. The energy saving potential of the proposed system was mainly realized in the MEE through energy recovery from exhaust air.

Acknowledgments

This work was supported by the Korean Agency for Infrastructure Technology Advancement (KAIA) grants (19CTAP-C141826-02), and by the Korean Institute of Energy Technology Evaluation and Planning (KETEP) (No. 20184010201710).

References

1 Jeong JW, Mumma SA, Bahnfleth WP. ASHRAE Trans **109** PART 2, 627–36 (2003).

2 Deng S, Lau J, Jeong JW. ASHRAE J **56**, 52–7 (2014).

3 Liu W, Lian Z, Radermacher R, Yao Y Energy **32**, 1749–60 (2007).

4 Xiao F, Ge G, Niu X. Appl Energy **88**, 43–9 (2011).

5 Bui DT, Kum Ja M, Gordon JM, Ng KC, Chua KJ. Energy **132**, 106–15 (2017).

6 El-Dessouky HT, Ettouney HM, Bouhamra W. Chemical Engineering Research and Design **78**, 199-1009 (2000).

7 Lin J, Thuan Bui D, Wang R, Chua KJ. Energy Procedia **142**, 3851–6 (2017).

8 Choi Y hee, Song D, Seo D, Kim J. Energy Build **172**,152–8 (2018).

9 Jang J, Kang EC, Lee HK, Jeong S, Park SR. Energies **11**, 1181 (2018).

10 Lee J, Lee DY. Int J Heat Mass Transf **65**, 173–9 (2013).

10 Hydeman M, Webb N, Sreedharan P, Blanc S. ASHRAE Trans **108** PART 2, 1118–27 (2002).